

Supplement of Atmos. Chem. Phys., 16, 11773–11786, 2016
<http://www.atmos-chem-phys.net/16/11773/2016/>
doi:10.5194/acp-16-11773-2016-supplement
© Author(s) 2016. CC Attribution 3.0 License.



Atmospheric
Chemistry
and Physics
Open Access
EGU

Supplement of

Isotopic composition for source identification of mercury in atmospheric fine particles

Qiang Huang et al.

Correspondence to: Jiubin Chen (chenjiubin@vip.gyig.ac.cn)

The copyright of individual parts of the supplement might differ from the CC-BY 3.0 licence.

Page S2	Calculation of Enrichment Factor and Principal Component Analysis
Page S3	Calculation of Secondary Organic Carbon
Page S5	Table S1
Page S6	Table S2
Page S7	Table S3
Page S8	Table S4
Page S9	Table S5
Page S10	Figure S1
Page S11	Figure S2
Page S12	Figure S3
Page S13	Figure S4
Page S14	References

Calculation of Enrichment Factor

The enrichment factor (EF) of a given element (e.g., Hg) in a sample is defined as the content of that element relative to its abundance in the upper continental crust (UCC) (Rudnick and Gao, 2003) in comparison with a process-insensitive element (e.g. Al, Fe, Ti, Si). In this study, we use Al as the process-insensitive element because Al is a main component of UCC and it presumably has little or no contribution from anthropogenic sources (Chen et al., 2014). The EF of an element of interest (C_{xx}) is calculated using the following equation:

$$EF_{xx} = (C_{xx}/C_{Al})_{\text{sample}} / (C_{xx}/C_{Al})_{\text{ucc}}$$

The EF values calculated for the PM_{2.5} samples are listed in [Table S4](#). In general, the elements with EF values between 5 and 10 in geochemical samples are considered to have significant contribution from non-crustal sources, whereas the elements with high EF values (>10) are essentially from anthropogenic activities (Chen et al., 2014).

Principal Component Analysis

Four factors are extracted from the Varimax rotated Principal Component Analysis, which accounted for 93% of the Explained Variance (Expl. Var.) of the entire data set. This finding is consistent with a previous report (Schleicher et al., 2015). The factor loadings are listed in [Table S5](#).

Factor **F-1** explains 39% of the total variance of the data, which is characterized by high loadings of the elements (Pb, Rb, Se, Zn, Tl, Cr, Cd, Fe and Ni) from mainly anthropogenic sources. After the phase-out of leaded gasoline in China since 1997, vehicle emission has not been the major emission source of Pb in airborne PM. Instead, coal combustion has since become the major source of Pb in PM (Zhang et al., 2009; Xu et al., 2012). Meanwhile, Se,

Cd and Zn with high contents were also considered mainly from coal combustion (Schleicher et al., 2012). Although many coal-fired power plants have been closed or replaced by gas-fired stations in Beijing, coal consumption is still huge in Beijing, particular in coal combustion for winter heating mainly used outside the 5th ring road of Beijing (Lin et al., 2016). Previous study showed that the petroleum refining and pollutant associated with petrochemical industry may be important sources of primary fine particles in Beijing, but they are not the main sources of PM_{2.5} (Lin et al., 2016). In addition to coal combustion, industrial activities (e.g. metallurgical processes) might also contribute to these element associations, as evidence by the highest EFs of Se, Cd, Pb, Zn, Tl and Cr in two dust samples from the smelting plant (Table S4). As a result, **F-1** is labeled as “mixed anthropogenic factor” mainly comprise coal combustion and nonferrous metal smelting. Factor **F-2** is characterized by high loading of Ca, Sr, Al and Mg which explains 24% of the total variance and indicated the lithogenic source contribution. Possible anthropogenic sources might be from construction activities as Ca, Sr, Al and Mg contents are high in cement materials, such as concrete mortar, lime or bricks (Schleicher et al., 2015). Additionally typical host minerals for these elements with low EFs (Table S4) may be from windblown dust (Visser et al., 2015). Collectively, Factor **F-1** and **F-2** can be labeled as a combination of coal combustion, nonferrous metal smelting and building materials that have high loading of Hg.

Factor **F-3** is characterized by high contents of Sb, Cu, PM_{2.5} and EC, accounting for 23% of the total variance. Since Sb and Cu in urban aerosols are mainly from brake wear of vehicles (Visser et al., 2015), this factor may be best referred to as “traffic emission factor”. Factor **F-4** is dominated by K and Na, which has been reported mainly from the biomass burning (Zheng et al., 2005a; Zheng et al., 2005b). Low loading of Hg in factors **F-3** and **F-4**

suggest traffic emission and biomass burning sources may be not the major contributors for PM_{2.5}-bound Hg.

Calculation of Secondary Organic Carbon

50 Secondary organic carbon (SOC) is frequently used to evaluate the efficiency of secondary aerosol production in the literature (Castro et al., 1999; Yu et al., 2004; Rengarajan et al., 2011). Here we use the EC-tracer method to estimate the SOC by employing the equation of $SOC = OC - EC * (OC/EC)_{min}$ (Castro et al., 1999; Cao et al., 2004; Yu et al., 2004; Rengarajan et al., 2011), and by assuming the minimum OC/EC ratio as the primary ratio
55 (Rengarajan et al., 2011). In this study, the $(OC/EC)_{min}$ of 2.02 observed for PM_{2.5} is used in the calculation.

Table S1. Total 23 PM_{2.5} samples were collected in four seasons from Beijing of China, and their sampling information, mercury concentrations and isotope compositions are displayed and their seasonal average and total average values are also given below.

Season	No.	Date	Rain (mm)	Arriving air mass	Sunshine duration (hr)	T ^a (°C)	RH ^b (%)	PM _{2.5} (µg/m ³)	THg (ng/g)	THg (pg/m ³)	OC (µg/m ³)	EC (µg/m ³)	OC (mg/g)	EC (mg/g)	δ ²⁰² Hg (‰)	Δ ¹⁹⁹ Hg (‰)	Δ ²⁰⁰ Hg (‰)	Δ ²⁰¹ Hg (‰)	Δ ²⁰⁴ Hg (‰)
Autumn	PM-01	2013-9-30	n ^c	SE	0	19.2	78	205	505	103	13.8	5.9	67	29	0.51	-0.53	0.17	-0.31	-0.23
	PM-02	2013-10-1	12	NW	3.6	18.5	81	56	319	18	4.8	1.6	86	29	-0.77	-0.07	0.06	-0.02	-0.81
	PM-03	2013-10-2	n	NW	10.9	17.1	50	61	461	28	5.8	2.7	95	44	-1.23	0.11	0.09	0.10	-0.80
	PM-04	2013-10-3	n	S	9.4	15.4	70	108	1520	164	7.2	3.5	66	33	0.08	0.02	0.10	0.09	-0.22
	PM-05	2013-10-4	n	SW	4.7	16.6	74	237	888	211	18.4	6.6	77	28	-0.31	-0.38	0.07	-0.48	-0.16
	PM-06	2013-10-5	n	S	5.3	18.3	74	308	680	210	33.2	9.2	108	30	-0.40	-0.29	0.06	-0.35	-0.25
	Average				17.5	71	163	728	122	13.9	4.9	83	32	-0.35	-0.19	0.09	-0.16	-0.41	
	1SD				1.4	11	103	433	87	10.8	2.8	16	6	0.61	0.25	0.04	0.25	0.31	
Winter	PM-07	2013-12-17	n	N	1.1	-0.6	49	70	516	36	7.6	2.5	108	36	-1.08	0.04	0.08	0.05	0.11
	PM-08	2013-12-18	n	N	7.7	-4.4	37	83	2200	182	12.3	4.1	149	49	-0.67	-0.12	0.02	-0.16	0.04
	PM-09	2013-12-19	n	N	8.3	-4.5	44	84	1350	113	15.7	5.1	186	61	-0.61	0.04	0.08	0.07	-0.19
	PM-10	2013-12-20	n	N	8	-2.8	36	67	925	62	9.3	3.3	140	50	-1.22	-0.09	0.03	-0.09	-0.07
	PM-11	2013-12-21	n	N	7	-2.4	36	120	1250	150	25.8	6.7	215	56	-0.25	-0.25	0.09	-0.19	-0.18
	PM-12	2013-12-22	n	NW	5.3	-3.3	52	174	1790	311	41.7	8.8	240	50	-0.46	-0.10	0.04	-0.12	-0.25
	Average				-3.0	42	100	1340	142	18.7	5.1	173	50	-0.72	-0.08	0.06	-0.07	-0.09	
	1SD				1.4	7	41	599	99	13.0	2.3	49	8	0.37	0.11	0.03	0.11	0.14	
Spring	PM-13	2014-4-22	n	SW	11.2	19.7	39	125	659	82	8.6	2.9	69	23	-0.51	0.40	0.10	0.36	-0.17
	PM-14	2014-4-23	n	S	8.8	20	60	140	505	71	8.0	2.3	57	16	-1.40	0.57	0.08	0.34	-0.18
	PM-15	2014-4-26	14	NW	8.8	15.6	63	91	252	23	5.3	1.5	58	17	-0.55	0.23	0.12	0.23	-0.43
	PM-16	2014-4-27	n	N	11.3	17.6	52	99	440	44	7.2	2.0	72	20	-1.13	0.14	0.09	0.07	-0.11
	PM-17	2014-4-28	n	N	11.3	18.8	42	111	485	54	8.6	2.7	77	24	-1.45	0.50	0.08	0.32	-0.08
	PM-18	2014-4-29	n	NW	10.9	19.3	41	126	679	85	8.9	3.5	71	28	-0.37	0.33	0.11	0.32	-0.39
	Average				18.5	50	115	503	60	7.7	2.5	67	21	-0.90	0.36	0.10	0.27	-0.23	
	1SD				1.7	10	18	157	24	1.4	0.7	8	5	0.48	0.16	0.02	0.11	0.15	
Summer	PM-19	2014-6-29	n	S	10.8	28.8	46	78	221	17	7.6	2.2	98	28	-2.18	0.54	0.10	0.33	0.41
	PM-20	2014-6-30	n	S	0	29.8	52	88	289	25	6.8	2.1	77	24	-0.73	0.11	0.12	0.03	-0.54
	PM-21	2014-7-1	49	S	0	28.8	85	72	150	11	2.8	1.2	40	16	-0.80	-0.05	0.16	-0.13	0.36
	PM-22	2014-7-2	n	SW	0.5	23.4	78	123	243	30	5.9	2.0	48	16	-0.84	0.06	0.08	0.06	-0.11
	PM-23	2014-7-3	n	SW	1.4	26.1	77	128	223	29	6.2	2.4	49	19	0.04	-0.04	0.17	-0.07	-0.77
		Average				27.4	68	98	225	22	5.9	2.0	53	18	-0.90	0.12	0.13	0.04	-0.13
	1SD				2.6	17	26	50	8	1.8	0.5	31	8	0.80	0.24	0.04	0.18	0.53	
Total average					14.6	57	120	720	90	11.8	3.7	98	32	-0.71	0.05	0.09	0.02	-0.22	
	1SD				11.4	17	61	551	80	9.6	2.3	54	14	0.58	0.29	0.04	0.23	0.31	

^a the daily average temperature; ^b the daily average relative humidity; ^c n is not detectable.

60 **Table S2.** Mercury concentrations and isotopic compositions for the 30 solid materials from different potential emission sources in China.

No.	Type	From	THg (ng/g)	$\delta^{202}\text{Hg}$ (‰)	$\Delta^{199}\text{Hg}$ (‰)	$\Delta^{200}\text{Hg}$ (‰)	$\Delta^{201}\text{Hg}$ (‰)	$\Delta^{204}\text{Hg}$ (‰)
TSP	Total suspended particle	Air of Yanqing district, northwestern Beijing	89	-0.74	0.18	0.01	0.06	-0.15
TS-01	Topsoil	Beijing, Olympic Park	408	-1.11	0.10	0.02	0.03	-0.09
TS-02	Topsoil	Beijing, Beihai Park	7747	-1.14	0.07	0.02	0.01	-0.10
TS-03	Topsoil	Beijing, the Winter Palace	40	-0.59	0.03	0.02	0.06	-0.24
TS-04	Topsoil	Beijing, Renmin University of China (RUC)	146	-0.77	0.04	0.04	0.08	-0.08
SM-D-01	Roof dust	Beijing, RUC	94	0.35	0.15	0.11	0.22	-0.44
SM-D-02	Road dust	Beijing, RUC	24	-0.79	0.18	0.10	0.27	-0.41
TS-05	Suburban topsoil	Shijiazhuang city	23	-1.37	-0.02	0.03	-0.04	-0.01
SM-D-03	Urban road dust	Shijiazhuang city	119	-0.75	0.04	0.06	0.07	-0.03
SM-D-04	Urban road dust	Shijiazhuang city	30	-0.66	-0.05	0.06	-0.03	-0.15
SM-D-05	Suburban road dust	Shijiazhuang city	70	-0.78	0.10	0.06	-0.03	0.10
SM-D-06	Suburban road dust	Shijiazhuang city	117	-0.77	0.07	0.07	0.03	0.03
CFPP-01	Feed coal	Coal-fired power plant -1 ^a	191	-1.26	0.02	0.03	0.04	-0.09
CFPP-02	Feed coal	Coal-fired power plant -2 ^b	54	-1.78	-0.27	-0.02	-0.25	0.11
CFPP-03	Bottom ash	Coal-fired power plant -1	2.1	-2.26	0.03	-0.01	-0.05	-0.09
CFPP-04	Bottom ash	Coal-fired power plant -2	0.35	0.48	-0.23	-0.04	-0.19	0.03
CFPP-05	Desulfurization gypsum	Coal-fired power plant -1	142	-0.58	0.02	0.01	0.00	0.01
CFPP-06	Desulfurization gypsum	Coal-fired power plant -2	6.8	0.62	-0.17	-0.03	-0.16	0.06
CFPP-07	Fly ash	Coal-fired power plant -1	332	-2.67	-0.20	-0.04	-0.21	-0.06
CFPP-08	Fly ash	Coal-fired power plant -2	875	-1.37	0.03	0.03	0.01	-0.04
SP-01	Blast furnace dust	Smelting plant ^c	113	-2.48	-0.11	0.00	-0.07	-0.07
SP-02	Sintering dust	Smelting plant	10800	-0.84	-0.17	-0.01	-0.13	-0.09
SP-03	Coke	Smelting plant	30	-0.72	-0.09	0.00	-0.03	-0.07
SP-04	Return powder	Smelting plant	1280	-0.42	-0.14	0.02	-0.12	-0.01
SP-05	Dust of blast furnace slag	Smelting plant	27	-0.42	-0.08	0.01	-0.07	-0.07
SP-06	Agglomerate	Smelting plant	29	-0.32	-0.12	-0.01	-0.07	0.07
CP-01	Coal-1	Cement plant ^d	471	-1.74	-0.09	0.01	-0.11	0.04
CP-02	Coal-2	Cement plant ^e	38	-1.55	-0.07	0.05	-0.13	-0.13
CP-03	Raw meal	Cement plant	241	-1.99	-0.07	0.00	-0.13	-0.07
CP-04	Sandstone	Cement plant ^e	13	-1.02	0.04	0.06	-0.03	-0.03
CP-05	Clay	Cement plant ^e	17	-1.79	-0.22	0.02	-0.29	-0.05
CP-06	Limestone	Cement plant ^e	13	-1.43	-0.07	-0.02	-0.03	0.08
CP-07	Desulfurization gypsum	Cement plant	1180	-1.47	-0.02	0.06	-0.02	-0.20
CP-08	Steel slag	Cement plant ^e	111	-1.02	0.00	-0.01	0.03	-0.03
CP-09	Sulfuric acid residue	Cement plant	278	-0.97	0.02	0.00	0.10	-0.11
CP-10	Cement clinker	Cement plant ^e	0.94	-1.18	0.00	0.01	0.06	-0.08

^a a coal-fire power plant from Hubei province; ^b a coal-fire power plant from Mongolia province; ^c a smelting plant from Qinghai province; ^d a cement plant from Sichuan province; ^e data have been published in our previous work (Wang et al., 2015).

Table S3. Concentrations of metal elements of the 14 PM_{2.5} samples from Beijing and 16 samples of the potential source materials.

Sample	Al*	Cd	Co	Cr	Cu	Fe*	Li	Ni	Pb	Rb	Sb	Se	Sr	Tl	V	Zn	Ca*	K*	Mg*	Na*
PM-01	3.06	13.4	7.86	64.9	367	5.64	9.19	28.6	832	27.9	76.4	29.0	36.3	12.0	32.2	2.02	5.64	5.68	1.26	4.04
PM-02	5.59	8.03	7.10	79.0	201	8.81	8.76	23.0	316	27.7	34.5	29.5	64.0	7.68	20.0	0.75	15.5	2.56	3.18	3.96
PM-03	9.04	10.6	10.1	114	225	11.8	14.3	37.9	449	27.8	37.0	20.2	108	6.96	25.1	1.10	32.1	5.66	11.2	3.36
PM-04	5.83	24.9	10.0	125	251	16.8	17.1	72.7	2710	115	27.0	85.9	72.7	22.0	50.8	4.28	18.4	15.1	6.41	6.61
PM-05	3.53	21.5	6.25	72.7	294	8.90	11.5	38.6	2130	76.1	49.0	62.5	44.7	19.8	27.9	3.50	7.09	12.8	2.23	3.90
PM-06	3.42	17.7	4.45	43.8	332	5.82	11.8	24.8	942	34.0	46.2	42.8	39.0	12.8	28.8	2.32	5.78	10.2	1.39	2.92
PM-08	10.1	14.9	13.4	85.6	217	14.0	16.5	62.5	709	43.7	42.3	30.6	172	11.0	33.2	1.39	34.8	10.4	8.32	8.34
PM-10	15.8	12.0	16.7	117	298	21.1	21.2	89.1	561	46.8	82.3	21.5	264	9.84	46.5	2.25	42.1	22.0	9.80	13.7
PM-11	8.73	18.0	11.6	88.5	341	11.4	30.5	48.1	1110	45.9	64.9	48.2	152	14.9	29.7	2.22	31.0	26.2	7.72	11.3
PM-12	7.97	19.2	12.4	83.9	269	10.8	22.2	45.3	1050	47.0	54.5	48.1	165	15.4	27.6	2.39	19.1	3.83	4.61	3.77
PM-14	5.85	25.9	4.77	55.3	182	7.18	14.4	25.6	873	39.1	17.3	55.0	63.2	13.1	26.1	1.80	14.5	10.3	4.85	3.69
PM-17	12.1	13.0	9.29	77.0	188	12.3	18.1	30.9	574	41.5	46.3	33.3	93.2	9.02	39.4	1.41	25.1	9.99	7.74	4.51
PM-19	5.03	19.5	6.19	75.4	316	9.60	13.5	32.2	1340	65.4	35.0	60.0	52.6	19.8	47.8	2.53	13.7	11.4	3.93	6.01
PM-22	1.51	21.2	2.72	47.2	412	3.10	7.49	18.0	734	25.4	25.4	34.7	19.5	14.9	18.7	2.01	2.92	4.26	-	3.60
SM-D-01	57.0	2.50	13.6	91.6	73.4	34.4	40.2	57.0	97.8	77.3	4.94	2.46	249	0.99	82.3	0.45	44.5	16.8	17.7	9.33
SM-D-02	61.6	0.57	5.11	27.1	7.72	15.5	15.6	9.50	19.6	89.7	0.47	0.69	515	0.60	48.9	0.05	27.5	29.0	8.74	17.6
SM-D-03	57.6	1.52	12.4	101	33.3	35.8	42.2	27.2	45.1	69.1	1.55	3.45	325	0.58	102	0.32	71.3	15.7	14.3	12.2
SM-D-05	49.0	1.09	10.0	77.5	56.3	31.4	27.8	22.0	42.2	74.7	1.46	1.65	278	0.62	71.6	0.26	71.7	17.8	20.0	9.39
TS-01	60.6	11.2	11.1	52.3	28.4	25.0	30.7	26.7	190	96.0	1.62	1.80	315	0.91	72.9	0.13	24.7	21.2	8.95	12.4
TS-02	50.9	0.96	10.0	56.0	50.8	22.2	28.4	22.7	93.5	82.5	1.82	2.48	423	0.74	64.2	0.11	61.8	17.7	9.36	9.83
TS-03	63.0	2.63	12.4	71.0	21.6	27.2	28.0	24.9	40.8	85.1	1.27	2.44	318	0.82	74.6	0.10	34.5	20.0	14.8	14.0
CFPP-07	113	3.18	39.8	111	138	55.0	71.0	76.5	86.2	233	3.14	6.04	369	4.23	237	0.24	10.3	21.8	3.89	6.55
CFPP-08	125	3.85	27.5	163	141	64.4	227	62.0	84.6	90.2	2.47	26.6	1680	1.53	348	0.16	32.2	19.0	5.95	3.74
CP-03	11.4	6.31	17.9	243	21.7	16.6	15.9	30.7	39.2	21.3	0.76	1.41	161	37.6	275	0.06	302	3.54	4.05	1.20
CP-04	40.8	1.16	7.99	36.6	14.3	20.8	27.6	18.1	14.6	60.5	1.43	2.95	77.6	0.65	54.4	0.05	39.8	11.7	6.87	0.79
CP-05	108	1.21	23.1	88.8	29.4	55.9	40.7	40.6	19.6	84.5	0.44	2.02	179	0.78	175	0.10	6.71	18.2	5.65	9.42
CP-10	20.9	3.43	23.3	584	38.3	28.8	26.9	54.8	50.8	33.1	1.28	1.39	222	0.14	637	0.13	446	5.35	6.33	0.87
SP-01	0.71	68800	1.43	2.34	132	1.61	4.18	1.33	369000	108	68.7	260	6.16	27.2	0.47	76.4	1.12	9.81	0.57	1.59
SP-02	0.08	94100	0.80	2.43	269	1.03	2.66	1.67	625000	109	262	401	4.35	2100	0.10	4.23	0.30	10.9	0.40	2.65
SP-04	10.3	11700	21.7	216	2840	99.1	9.05	90.1	400000	24.3	228	92.0	281	61.3	13.8	41.1	43.3	3.01	7.12	2.58

* units of µg/g, others with units of ng/g.

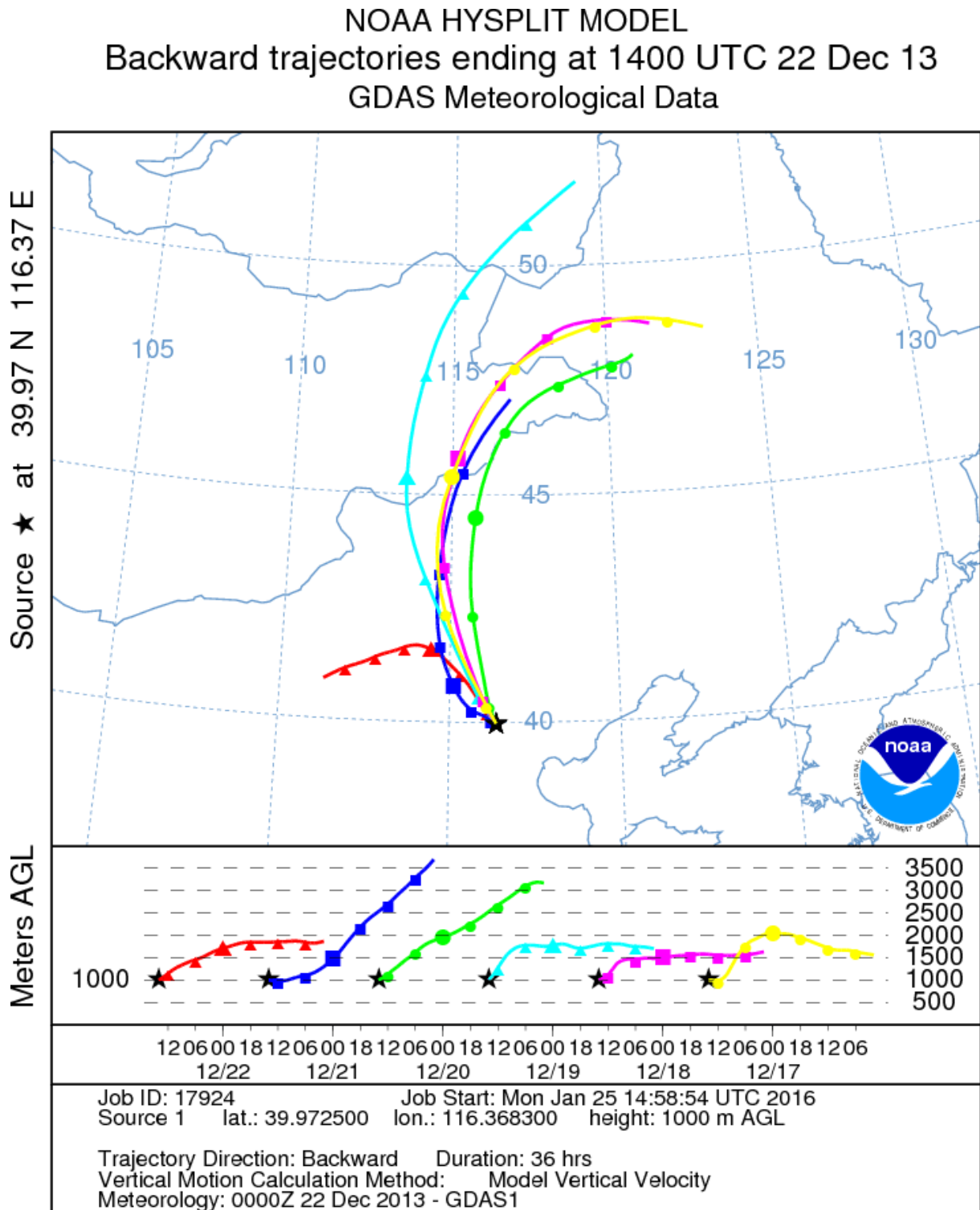
65 **Table S4.** The calculated enrichment factors (EFs) in PM_{2.5} samples and potential source materials.

Sample	Cd	Co	Cr	Cu	Fe	Li	Ni	Pb	Rb	Sb	Se	Sr	Tl	V	Zn	Ca	K	Mg	Na	Hg
PM-01	3962	12	19	349	4	10	16	1305	9	5089	8597	3	354	9	803	6	7	2	4	269
PM-02	1302	6	13	105	3	5	7	271	5	1260	4787	3	125	3	163	9	2	3	2	93
PM-03	1059	5	11	72	3	5	7	238	3	835	2027	3	70	2	149	11	2	7	1	83
PM-04	3874	8	19	125	6	10	22	2230	19	944	13339	3	342	7	893	10	9	6	4	424
PM-05	5535	8	18	243	5	11	19	2897	21	2829	16060	3	507	7	1209	6	13	3	4	411
PM-06	4692	6	11	283	4	12	13	1321	10	2754	11344	3	338	7	826	5	10	2	3	324
PM-08	1330	6	7	62	3	6	11	335	4	852	2733	4	98	3	167	11	4	4	3	354
PM-10	688	5	7	55	3	5	10	170	3	1061	1230	4	56	2	173	8	5	3	3	95
PM-11	1873	6	9	114	3	12	10	611	5	1515	5003	4	154	3	309	11	11	5	4	234
PM-12	2183	7	9	98	3	9	10	631	6	1394	5466	5	175	3	365	8	2	3	2	366
PM-14	4010	4	8	91	3	8	8	716	6	603	8525	3	203	4	375	8	6	5	2	141
PM-17	976	4	6	45	2	5	4	228	3	782	2500	2	68	3	142	7	3	4	1	66
PM-19	3504	6	13	183	4	9	11	1277	13	1417	10799	3	357	8	611	9	8	4	4	72
PM-22	12723	9	28	796	4	17	21	2333	16	3438	20869	3	892	10	1625	6	10	—	8	263
SM-D-01	40	1	1	4	1	2	2	8	1	18	39	1	2	1	10	2	1	2	1	3
SM-D-02	8	0	0	0	1	1	0	2	1	2	10	2	1	1	1	1	2	1	1	1
SM-D-03	24	1	2	2	1	2	1	4	1	5	54	1	1	1	7	4	1	1	1	1
SM-D-05	20	1	1	3	1	2	1	4	1	6	31	1	1	1	6	5	1	2	1	4
TS-01	168	1	1	1	1	2	1	15	2	5	27	1	1	1	3	1	1	1	1	11
TS-02	17	1	1	3	1	2	1	9	2	7	44	2	1	1	3	4	1	1	1	248
TS-03	38	1	1	1	1	2	1	3	1	4	35	1	1	1	2	2	1	1	1	1
CFPP-07	25	2	1	4	1	2	1	4	2	6	48	1	3	2	3	0	1	0	0	5
CFPP-08	28	1	1	3	1	6	1	3	1	4	192	3	1	2	2	1	1	0	0	11
CP-03	502	7	19	6	3	5	5	16	2	14	112	4	299	20	6	84	1	2	0	34
CP-04	26	1	1	1	1	2	1	2	1	7	65	0	1	1	1	3	1	1	0	1
CP-05	10	1	1	1	1	1	1	1	1	1	17	0	1	1	1	0	1	0	0	0
CP-10	149	5	25	5	3	4	5	12	2	12	60	3	1	26	8	68	1	2	0	0
SP-01	87570416	9	3	541	5	20	3	2488020	147	19694	331752	2	3467	1	130705	5	48	4	8	258
SP-02	1095027659	48	28	10070	28	116	37	38515102	1361	686994	4661642	14	2437629	1	66158	12	490	28	114	226070
SP-04	1028376	10	19	802	20	3	15	186101	2	4515	8098	7	540	1	4863	13	1	4	1	203

Table S5. Factor (F) loadings of the extracted factors for PM_{2.5} samples from Beijing urban area of China. Four factors account for 93% of the Explained Variance (Expl. Var.).

	F-1	F-2	F-3	F-4
Hg	0.59	0.62	0.38	-0.14
Pb	0.97	0.05	0.14	0.13
Rb	0.97	0.05	0.14	0.13
Se	0.89	0.03	0.35	0.20
Zn	0.86	0.03	0.46	0.18
Tl	0.85	0.03	0.49	0.17
Cr	0.79	0.31	0.45	0.04
Cd	0.78	0.06	0.48	0.21
Fe	0.77	0.53	0.23	0.12
Ni	0.75	0.46	0.34	0.11
V	0.66	0.02	0.63	0.22
Ca	-0.13	0.96	-0.14	0.22
Sr	0.05	0.93	0.23	-0.09
Al	0.10	0.85	0.21	0.13
Mg	0.03	0.84	-0.38	0.22
Co	0.38	0.67	0.58	-0.09
Li	0.42	0.62	0.49	0.29
Sb	0.34	0.13	0.89	0.16
Cu	0.50	-0.02	0.83	0.24
PM _{2.5}	0.60	0.04	0.74	0.19
EC	0.42	0.48	0.72	0.10
K	0.53	0.18	0.27	0.78
Na	0.26	0.47	0.34	0.66
% of Expl. Var.	39	24	23	7

Figure S1. NOAA-HYSPLIT model (<http://ready.arl.noaa.gov>) results illustrate air mass back trajectories for PM_{2.5} samples collected in Winter.



70 **Figure S2.** NOAA-HYSPLIT model ([http://ready.arl.noaa.gov.](http://ready.arl.noaa.gov)) results illustrated air mass back trajectories for PM_{2.5} samples collected in Autumn (from 30 Sep to 5 Oct 2013). $\Delta^{199}\text{Hg}$ values were also land-marked on the corresponding trajectories.

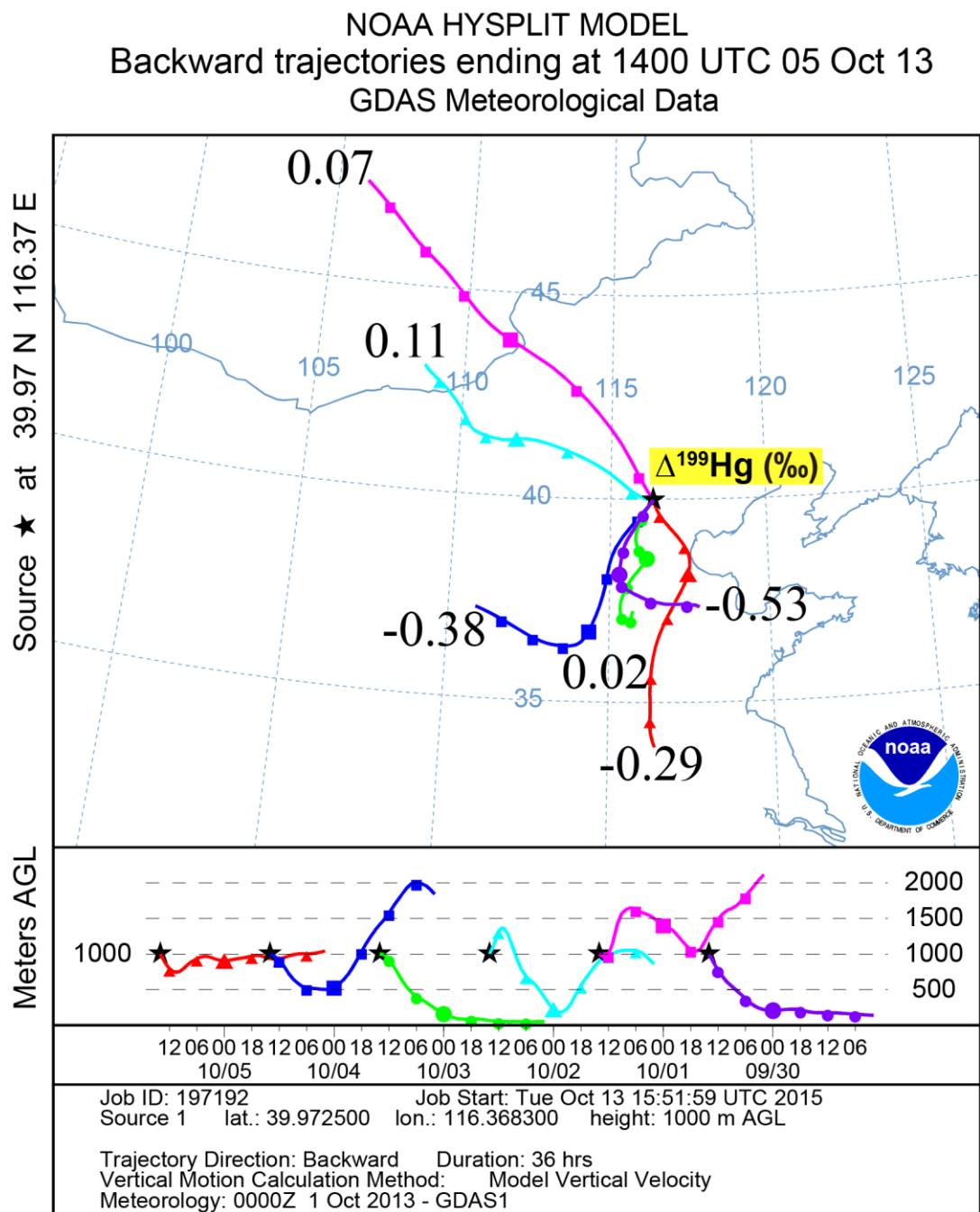


Figure S3. NOAA-HYSPLIT model (<http://ready.arl.noaa.gov>) results illustrate air mass

75 back trajectories for PM_{2.5} samples collected in Spring.

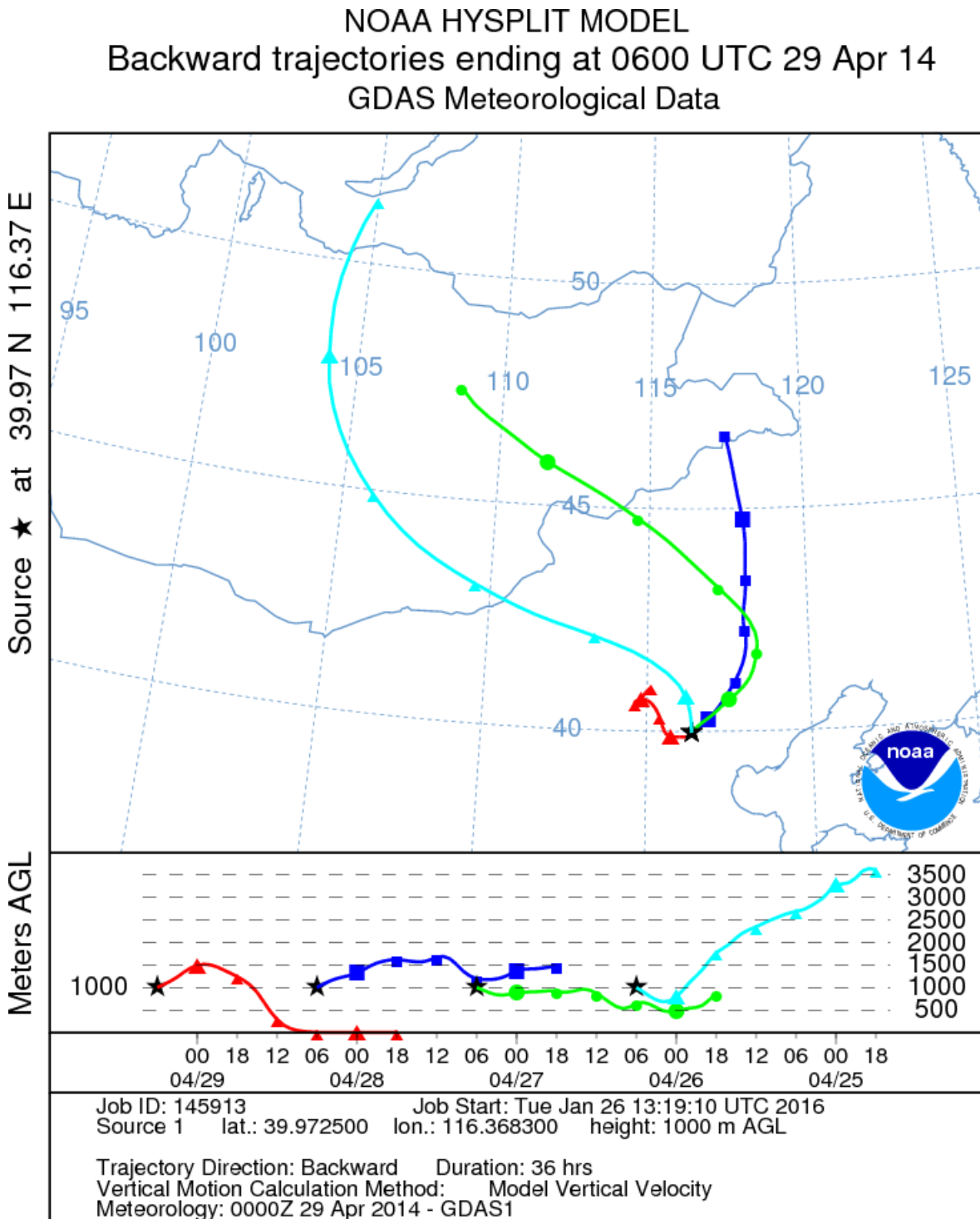
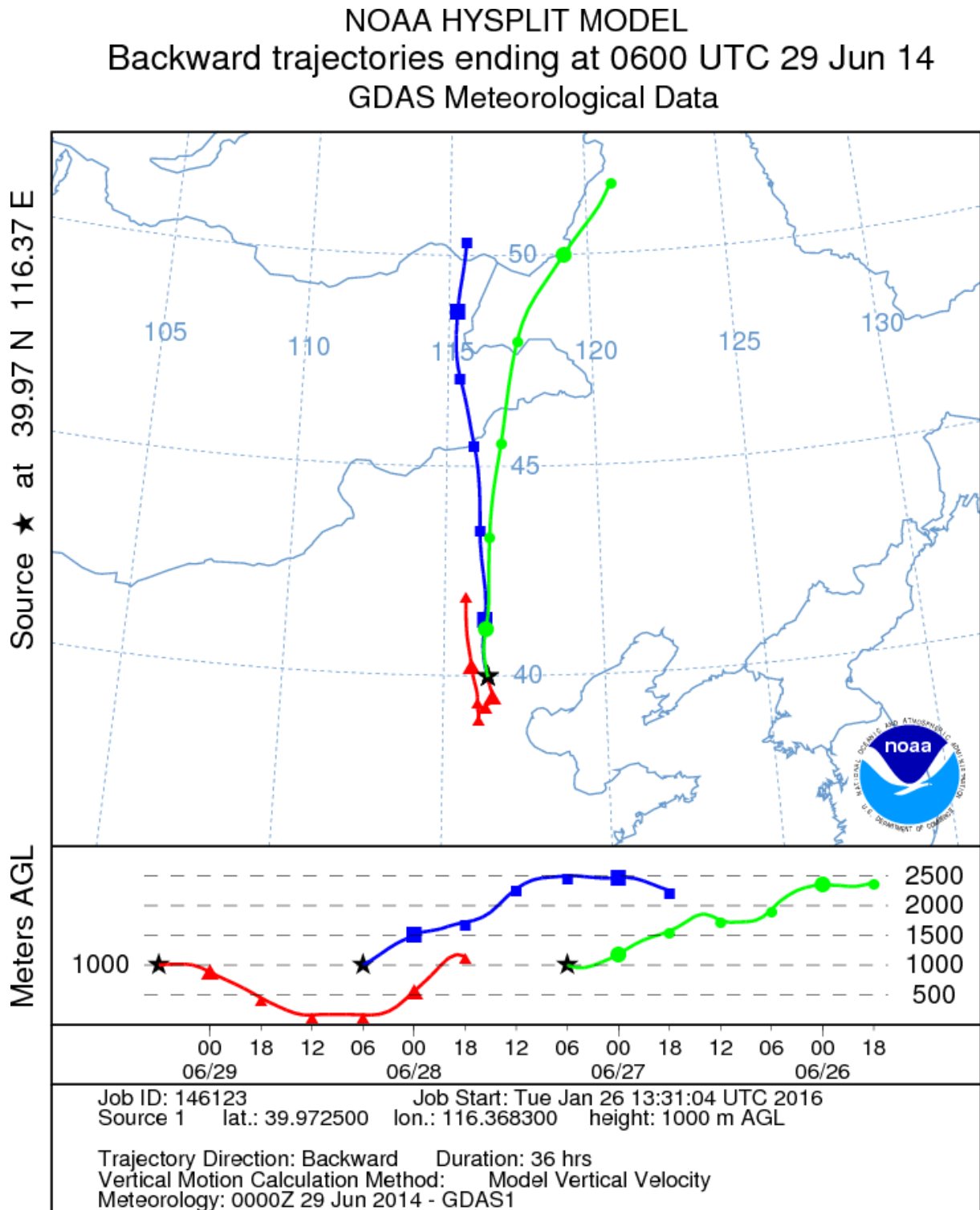


Figure S4. NOAA-HYSPLIT model (<http://ready.arl.noaa.gov>) results illustrate air mass back trajectories for PM_{2.5} samples collected in early Summer.



80 **REFERENCES**

- Cao, J. J., Lee, S. C., Ho, K. F., Zou, S. C., Fung, K., Li, Y., Watson, J. G., and Chow, J. C.: Spatial and seasonal variations of atmospheric organic carbon and elemental carbon in Pearl River Delta Region, China, *Atmos. Environ.*, 38, 4447-4456, <http://dx.doi.org/10.1016/j.atmosenv.2004.05.016>, 2004.
- 85 Castro, L. M., Pio, C. A., Harrison, R. M., and Smith, D. J. T.: Carbonaceous aerosol in urban and rural European atmospheres: Estimation of secondary organic carbon concentrations, *Atmos. Environ.*, 33, 2771-2781, [http://dx.doi.org/10.1016/S1352-2310\(98\)00331-8](http://dx.doi.org/10.1016/S1352-2310(98)00331-8), 1999.
- Chen, J. B., Gaillardet, J., Bouchez, J., Louvat, P., and Wang, Y. N.: Anthropophile elements in river sediments: Overview from the Seine River, France, *Geochem. Geophys. Geosyst.*,
90 15, 4526-4546, 2014.
- Lin, Y.-C., Hsu, S.-C., Chou, C. C.-K., Zhang, R., Wu, Y., Kao, S.-J., Luo, L., Huang, C.-H., Lin, S.-H., and Huang, Y.-T.: Wintertime haze deterioration in Beijing by industrial pollution deduced from trace metal fingerprints and enhanced health risk by heavy metals, *Environ. Pollut.*, 208, 284-293, 2016.
- 95 Rengarajan, R., Sudheer, A., and Sarin, M.: Aerosol acidity and secondary organic aerosol formation during wintertime over urban environment in western India, *Atmos. Environ.*, 45, 1940-1945, 2011.
- Rudnick, R., and Gao, S.: Composition of the continental crust, *Treatise on Geochemistry*, 3, 1-64, 2003.
- 100 Schleicher, N., Norra, S., Chen, Y., Chai, F., and Wang, S.: Efficiency of mitigation measures to reduce particulate air pollution: A case study during the Olympic Summer Games 2008 in Beijing, China, *Sci. Total Environ.*, 427-428, 146-158, <http://dx.doi.org/10.1016/j.scitotenv.2012.04.004>, 2012.
- Schleicher, N. J., Schäfer, J., Blanc, G., Chen, Y., Chai, F., Cen, K., and Norra, S.:
105 Atmospheric particulate mercury in the megacity Beijing: Spatio-temporal variations and source apportionment, *Atmos. Environ.*, 109, 251-261, doi: 10.1016/j.atmosenv.2015.03.018, 2015.
- Visser, S., Slowik, J., Furger, M., Zotter, P., Bukowiecki, N., Dressler, R., Flechsig, U., Appel,

- 110 K., Green, D., and Tremper, A.: Kerb and urban increment of highly time-resolved trace
elements in PM 10, PM 2.5 and PM 1.0 winter aerosol in London during ClearfLo 2012,
Atmos. Chem. Phys., 15, 2367-2386, 2015.
- Wang, Z., Chen, J., Feng, X., Hintelmann, H., Yuan, S., Cai, H., Huang, Q., Wang, S., and
Wang, F.: Mass-dependent and mass-independent fractionation of mercury isotopes in
precipitation from Guiyang, SW China, *C. R. Geosci.*, 347, 358-367, doi:
115 10.1016/j.crte.2015.02.006, 2015.
- Xu, H., Cao, J., Ho, K., Ding, H., Han, Y., Wang, G., Chow, J., Watson, J., Khol, S., and
Qiang, J.: Lead concentrations in fine particulate matter after the phasing out of leaded
gasoline in Xi'an, China, *Atmos. Environ.*, 46, 217-224, 2012.
- Yu, S., Dennis, R. L., Bhave, P. V., and Eder, B. K.: Primary and secondary organic aerosols
120 over the United States: Estimates on the basis of observed organic carbon (OC) and
elemental carbon (EC), and air quality modeled primary OC/EC ratios, *Atmos. Environ.*, 38,
5257-5268, <http://dx.doi.org/10.1016/j.atmosenv.2004.02.064>, 2004.
- Zhang, Y., Wang, X., Chen, H., Yang, X., Chen, J., and Allen, J. O.: Source apportionment of
lead-containing aerosol particles in Shanghai using single particle mass spectrometry,
125 *Chemosphere*, 74, 501-507, 2009.
- Zheng, M., Salmon, L. G., Schauer, J. J., Zeng, L., Kiang, C. S., Zhang, Y., and Cass, G. R.:
Seasonal trends in PM_{2.5} source contributions in Beijing, China, *Atmos. Environ.*, 39,
3967-3976, doi: 10.1016/j.atmosenv.2005.03.036, 2005a.
- Zheng, X., Liu, X., Zhao, F., Duan, F., Yu, T., and H, C.: Seasonal characteristics of biomass
130 burning contribution to Beijing aerosol, *Sci. China Ser. B*, 48, 481-488, doi:
10.1360/042005-15, 2005b.